Section A-Research paper
ISSN 2063-5346

Hall and Ion slip effects on MHD free convective rotating flow bounded by the semi - infinite vertical porous surface

Kamala Pratapa[1], Siva Reddy Sheri[2*]
[2]Department of Mathematics, GITAM University, Hyderabad Campus, Telangana, India
[1] Department of Mathematics, CMRCET, Kandlakoya, Medchal, Telangana, India
[*]Corresponding author email: sreddy7@yahoo.co.in

Abstract: In this paper we investigated Hall and ion slip effects, thermal diffusion and thermal radiation effects on mass and heat transfer transport on magnetohydrodynamical micro polar free convective flow of fluid bounded by partly-infinite non reflective plate with suction and rotation. Plate oscillates with constant frequency in time hence solutions for boundary layer are of oscillatory method. The solution is obtained by Finite Element Method. By graphical representations impacts of velocity, temperature and concentration inside boundary layer are represented.

Keywords: Rotating frame, micro polar fluid, mass transfer, suction, dufour effect.

1. Introduction

In viscous medium randomly oriented particles are suspended that rotate and influence hydrodynamics of flows; these are micro polar fluids they are dominantly non-Newtonian fluids. Revolving fluids study is very significant because of its presence as naturally magnificent behavior and technological solutions acted by Coriolis force.

Eringen[1] facilitated for study of complex fluids like polymer fluid, blood and colloidal fluids. Rotating fluids have natural phenomena and technical situations governed by coriolis forces. Rotating fluids are essential feature in areas like Atmospheric Sciences, Meteorology and Oceanography. The study of rotating fluids in viscous and incompressible fluids are considered for various research problems. Compared to inertial and viscous forces coriolis forces are researched extensively. It is also noticed that coriolis forces and magnetism share many resemblances. Ellahi et al[2] studied ion-slip and Hall effects on Jeffrey liquids flowing tubes which are not uniform. Bhatti et al[3] studied ion-slip and Hall effects and flow of blood patterns along with zero Reynolds number. Srinivasacharya and shafeeurahman[4] studied sensory Nano fluids for ion-slip and Hall effects, these fluids have effect of MHD. Jitendra and Srinivas[5] studied ion-slip and Hall effects on gyratory liquid passing over exponentially accelerated vertical plate. Veera Krishna and Chamkha[6] studied Nano fluids for ion-slip and Hall effects, diffusion thermo along with radiation absorption effects over rotating convective MHD fluids flowing with constant temperature over permeable plate. Sara and Bhatti[7] studied non-Newtonian MHD peristaltic flows for ion-slip and Hall effects.

Ch. Vijaya Bhaskar et al.[14] MHD casson fluid‘s ramped wall temperature and ramped surface concentration was investigated. M. Ijaz Khan et al. [15] Flow nature of Nano fluid with gyrotic microorganism in Walter – B is studied. M.K. Nayak et al. Krishna et al.[16] studied unsteady hydro magnetic convective gyrating flows in exponentially accelerated surface for Hall and ion-slip effects. Singh and Vishwanath[17] studied magnetically influenced convective heated angular surface in constant permeable base. The flow is steady of Walters’-B effected by thermal and mass concentration buoyancy forces, Hall and ion-slip effects are studied. Veera Krishna[18] studied Hall and ion slip effects for revolving convective MHD flanked by partially never ending upright permeable surfaces. Veera Krishna et al.[19] studied consequences Hall and ion slip on gyrating MHD flow of small entity in ciliary thrust. Olanrewaju and Makinde[20] investigated the hydro magnetic flow of a novel type of a water based Nano fluid containing nanoparticles and microorganisms past a permeable vertical moving plate. Pit R. Hervet H and Leger. L[21] studied numerically the behavior of a water−based Nano fluid containing motile microorganisms passing an isothermal nonlinear stretching sheet in the presence of a non−uniform magnetic field. Sheikholeslami, M.,

Darzi, M. and Li, Z[22] modeled the alumina Nano fluid magnetohydrodynamic flow through a permeable enclosure using CVFEM. The results show that the Lorentz forces reinforce the conduction mechanism. The Brownian motion and shape factor influence the viscosity and thermal conductivity of alumina.

Raza, Rohni, Omar and Awais[23] had done a bit of work on Nano fluids in a rotating channel wherein MHD three-dimensional flow was investigated. The problem was solved by numerical strategy. Investigations of the fluid flow problems in a channel with permeable expanding or contracting walls have attracted most of the researchers due to the vast applications in the fields of chemical, biomedical, engineering and science. The blood flow in vessels, artificial kidneys and the air flow in respiratory system are most prominent examples

Taking references from the literature survey this paper studies mass transfer, thermal radiation and thermo diffusion on MHD free convective micro polar flows surrounded by partly-infinite porous plate. Suction ion-slip and Hall effects are studied.

2. Formulation and Solution of the Problem

Unsteady incompressible, electrically conducting MHD micro polar fluids along with thermo diffusion and thermal radiation on semi-infinitely porous moving plate were considered for studying ion-slip and Hall effects, suction. This said flow is subjected to steady magnetic field B_0 in presence of concentration along with thermal buoyancy. Then x-axis is considered along the plate and z-axis is orthogonal to it, Figure 1. is representation

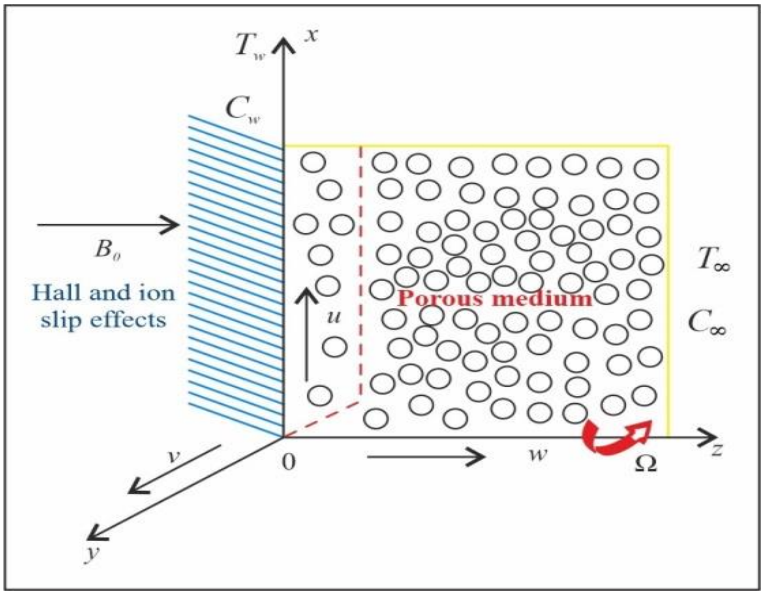

Figure1. Geometrical configuration

The governing equations[8] are

$$\frac{\partial w}{\partial z} = 0 \tag{1}$$

$$\frac{\partial u}{\partial t} + w\frac{\partial u}{\partial z} - 2\Omega v = (\nu + \nu_r)\frac{\partial^2 u}{\partial z^2} + \frac{B_0 J_y}{\rho} - \frac{\nu}{k}u + g\beta_T(T - T_\infty) + g\beta_C(C - C_\infty) - \nu_r\frac{\partial \bar{\omega}_2}{\partial z} \tag{2}$$

$$\frac{\partial v}{\partial t} + w\frac{\partial v}{\partial z} + 2\Omega u = (\nu + \nu_r)\frac{\partial^2 v}{\partial z^2} - \frac{B_0 J_x}{\rho} - \frac{\nu}{k}v + \nu_r\frac{\partial \bar{\omega}_1}{\partial z} \tag{3}$$

$$\frac{\partial \bar{w}_1}{\partial t} + w\frac{\partial \bar{\omega}_1}{\partial z} = \frac{\wedge}{\rho j}\frac{\partial^2 \bar{\omega}_1}{\partial z^2} \tag{4}$$

$$\frac{\partial \bar{w}_2}{\partial t} + w\frac{\partial \bar{\omega}_2}{\partial z} = \frac{\Lambda}{\rho j}\frac{\partial^2 \bar{\omega}_2}{\partial z^2} \quad (5)$$

$$\frac{\partial T}{\partial t} + w\frac{\partial T}{\partial z} = \frac{k_1}{\rho C_p}\frac{\partial^2 T}{\partial z^2} - \frac{1}{\rho C_p}\frac{\partial q_r}{\partial z} + \frac{k_T D_m}{\rho C_p}\frac{\partial^2 C}{\partial z^2} \quad (6)$$

$$\frac{\partial C}{\partial t} + w\frac{\partial C}{\partial z} = D_m\frac{\partial^2 C}{\partial z^2} \quad (7)$$

The limiting conditions are

$u = v = 0\,,\ \bar{\omega}_1 = \bar{\omega}_2 = 0,\qquad \mathrm{C} = C_\infty\ \mathrm{T} = T_\infty$ for $t \le 0$, (8)

$u = U_r(1 + \frac{\varepsilon}{2}(e^{int} + e^{-int}))$, $v = 0$, $\bar{\omega}_1 = -\frac{i}{2}\frac{\partial v}{\partial z}$, $\bar{\omega}_2 = -\frac{i}{2}\frac{\partial u}{\partial z}$, $-k_1\frac{\partial T}{\partial z} = q_\omega$, $-D_m\frac{\partial C}{\partial z} = M_\omega$ at z=0

$u = v = 0\,,\ \bar{\omega}_1 = \bar{\omega}_2 = 0$, $\mathrm{C} = C_\infty\ \mathrm{T} = T_\infty$ while $z \to \infty$ for $t > 0$ (9)

By equation (1)

$w = -w_0$, w_0 is suction velocity. (10)

Ganapathy[9] is base for oscillatory plate speed.

Rossland approximation[10] leading to the emission of radiation heat flux q_r is transformed to

$$q_r = -\frac{4\sigma^*}{3k^*}\frac{\partial T^4}{\partial z} \quad (11)$$

Temperature boundary conditions are linear with time and with residual temperature T^4 .

By neglecting higher powers using Taylor series about T_∞

We consider $T^4 \cong 4T_\infty^3 T - 3T_\infty^4$ (12)

Similar to gray fluids absorbent /emitting fluids are considered but medium is not-scattering

$$\frac{\partial q_r}{\partial z} = -\frac{16T_\infty^3\sigma^*}{3k^*}\frac{\partial^2 T}{\partial z^2} \quad (13)$$

The collision frequency of atom and electron is high hence ion slip and hall current cannot be neglected. By generalized ohm's law and including Hall and ion slip[11] effect the influence of large magnetic field is

$$J = \sigma(E + V \times B) - \frac{\omega_e\tau_e}{B_0}(J \times B) + \frac{\omega_e\tau_e\beta_i}{B_0^2}((J \times B) \times B) \quad (14)$$

Further assumption $\omega_e\tau_e \sim O(1)$ and $\omega_i\tau_i \ll 1$,

The pressure gradient of electron and effects of thermo-electric are neglected implies E=0 results

$$(1 + \beta_e\beta_i)J_x + \beta_e J_y = \sigma B_0 v \quad (15)$$

$$(1 + \beta_e\beta_i)J_y - \beta_e J_x = -\sigma B_0 u \quad (16)$$

by solving Eqs. (15) and (16) we get

$$J_x = \sigma B_0\left(\frac{\beta_e}{(1+\beta_e\beta_i)^2+\beta_e{}^2}u + \frac{1+\beta_e\beta_i}{(1+\beta_e\beta_i)^2+\beta_e{}^2}v\right) \quad (17)$$

$$J_y = -\sigma B_0\left(\frac{\beta_e}{(1+\beta_e\beta_i)^2+\beta_e{}^2}v - \frac{1+\beta_e\beta_i}{(1+\beta_e\beta_i)^2+\beta_e{}^2}u\right) \quad (18)$$

The non-dimensional variables are

$$u^* = \frac{u}{U_r}\ ,\ v^* = \frac{v}{U_r}\ ,\ z^* = \frac{zU_r}{v}\ ,t^* = \frac{tU_r^2}{v}\ n^* = \frac{nv}{U_r{}^2}\ ,\ \bar{\omega}_1{}^* = \frac{\bar{\omega}_1 v}{U_r^2}\ ,\ \bar{\omega}_2{}^* = \frac{\bar{\omega}_2 v}{U_r^2}\ ,\ \theta = \frac{k_1(\mathrm{T}-T_\infty)}{q_w}$$

$$\phi = \frac{D_m(\mathrm{C}-C_\infty)}{M_w}\ ,\ R = \frac{\Omega v}{U_r{}^2}\ ,\ M = \frac{B_0}{U_r}\sqrt{\frac{\sigma\nu}{\rho}}\ ,\ Pr = \frac{\mu\rho C_p}{k_1}\ ,\ Sc = \frac{\nu}{D_m}\ ,\ Gr = \frac{\nu g\beta_T q_w}{k_1 U_r^3}\ ,Gm = \frac{\nu g\beta_C M_w}{D_m U_r^3},\quad N = \frac{4T^3\sigma^*}{k_1 k^*}\ ,\quad K = \frac{kU_r^2}{\nu^2}\ ,\quad Du = \frac{k_T^2 K_T M_w}{q_w\rho c\mu}\ ,\ S = \frac{w_0}{U_r}\ ,\ \delta = \frac{\Lambda}{\mu j}\ ,\ \lambda = \frac{\nu_r}{\nu}$$

Governing equations reduces to

$$\frac{\partial u}{\partial t} - S\frac{\partial u}{\partial z} - 2\mathrm{R}v =$$
$$(1+\lambda)\frac{\partial^2 u}{\partial z^2} + M^2\left(\frac{\beta_e}{(1+\beta_e\beta_i)^2+\beta_e{}^2}v - \frac{1+\beta_e\beta_i}{(1+\beta_e\beta_i)^2+\beta_e{}^2}u\right) - \frac{1}{K}u + Gr\theta + \mathrm{Gm}\phi - \lambda\frac{\partial\bar{\omega}_2}{\partial z} \quad (19)$$
$$\frac{\partial v}{\partial t} - S\frac{\partial v}{\partial z} + 2\mathrm{R}u = (1+\lambda)\frac{\partial^2 v}{\partial z^2} - M^2\left(\frac{1+\beta_e\beta_i}{(1+\beta_e\beta_i)^2+\beta_e{}^2}v + \frac{\beta_e}{(1+\beta_e\beta_i)^2+\beta_e{}^2}u\right) - \frac{1}{K}v + \lambda\frac{\partial\bar{\omega}_1}{\partial z} \quad (20)$$
$$\frac{\partial\bar{w}_1}{\partial t} - S\frac{\partial\bar{\omega}_1}{\partial z} = \delta\frac{\partial^2\bar{\omega}_1}{\partial z^2} \quad (21)$$
$$\frac{\partial\bar{w}_2}{\partial t} - S\frac{\partial\bar{\omega}_2}{\partial z} = \delta\frac{\partial^2\bar{\omega}_2}{\partial z^2} \quad (22)$$
$$\frac{\partial\theta}{\partial t} - S\frac{\partial\theta}{\partial z} = \frac{1}{Pr}\left(1+\frac{4N}{3}\right)\frac{\partial^2\theta}{\partial z^2} + Du\frac{\partial^2\phi}{\partial z^2} \quad (23)$$
$$\frac{\partial\phi}{\partial t} - S\frac{\partial\phi}{\partial z} = \frac{1}{Sc}\frac{\partial^2\phi}{\partial z^2} \quad (24)$$

The changed boundary conditions are

$u = v = 0, \bar{\omega}_1 = \bar{\omega}_2 = 0, \phi = 0, \theta = 0,$ for $t \le 0$, (25)

$u = 1 + \frac{\varepsilon}{2}(e^{int} + e^{-int})$, $v = 0$, $\bar{\omega}_1 = -\frac{i}{2}\frac{\partial v}{\partial z}$ $\bar{\omega}_2 = -\frac{i}{2}\frac{\partial u}{\partial z}$, $\frac{\partial\phi}{\partial z} = -1$, $\frac{\partial\theta}{\partial z} = -1$, for z=0

$u = 0 = v$, $\bar{\omega}_1 = \bar{\omega}_2 = 0, = 0, \theta = 0$, as $z \to \infty$ for $t > 0$ (26)

3. Solution of the problem

Equations (19), (20), (21), (22), (23), (24) nonlinear equation and their boundary conditions (25), (26) are numerically solved for concentration, temperature and velocity distributions. The procedure is discussed by Bathe[25] and Reddy[26].The FEM is applied to get accurate and reliable solutions for coupled nonlinear equation and their boundary conditions. The fundamental steps are

1. Domain elements Discretization
   The element of domain is divided into finite number of sub intervals which is known as discretization. Each sub interval is now a finite element. The group of these sub intervals is termed as finite mesh.
2. Finite element equation derivation
   The finite element equations derivation of consists of three steps
   - Construction of variation formulation for differential equation.
   - Assumption of approximate solution for typical finite element.
   - Derivation of finite element equation by substituting the solution in variation formulation.
3. Assembly for element equation
   The results obtained by above procedure are assembled by subjecting to inter-element continuity conditions. This results to a large number of algebraic equations making into global finite element model governing whole flow domain.
4. The boundary conditions of equation (25), (26) applied for these assembled equations.
5. The final set of equations is solved directly or by iterative numerical methods. Numerical solutions of these equations were obtained by MATLAB. By changing the values of velocity, temperature and concentration the stability and convergence of finite element method was tested. The results were more than satisfactory

4. Results and Discussion

We have defined governing equations for free convective MHD incompressible micro-polar fluids flowing over partly-infinite perpendicular permeable moving plate inside permeable rotating frame. We studied graphically thermal radiation, thermo-diffusion, ion slip and Hall effects for mass heat and transfer flows. The solutions were obtained numerically for distribution of temperature, concentration, velocity and micro rotation over boundary layer. Different parameters considered are $M = R = K = \delta = N = 0.5$,$Du = 0.5$,$Gm = 5$,$Gr = 5$, ,$Pr = 0.71$,$Sc = 0.22, \lambda = 0.2$, ,$S = 1$,$n = \pi/6$,$\beta_e = 1$, $\beta_i = 0.3$, $t = 0.2$.

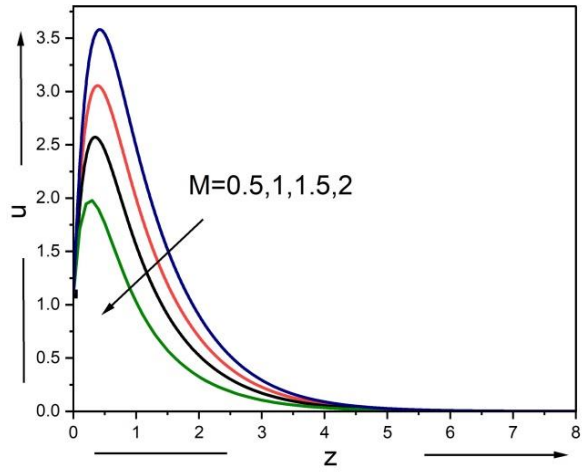

2(A) Velocity portrait for different values of M

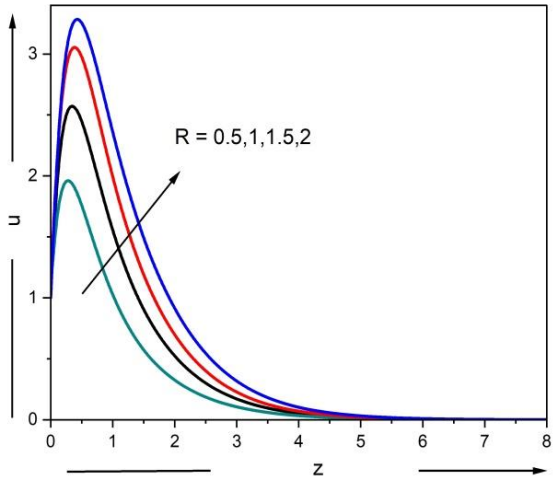

2(B) Velocity portrait for different values of R

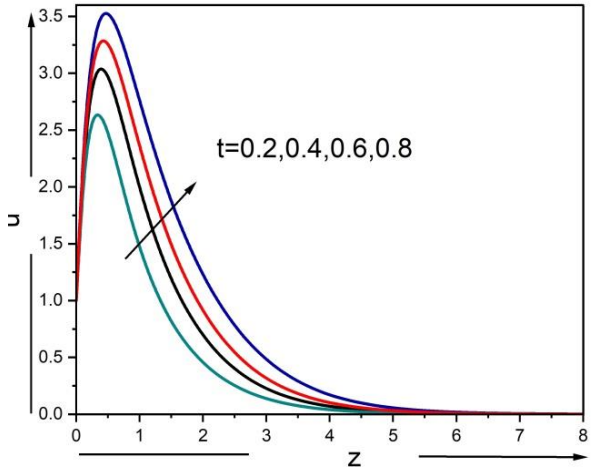

2(C) Velocity potrait for different values of t

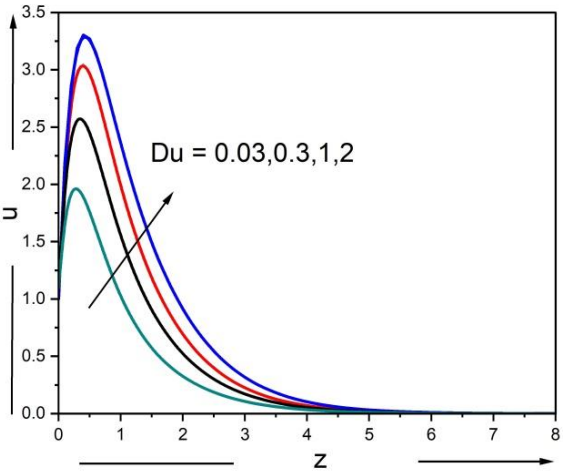

2(D) Velocity potrait for different values of Du

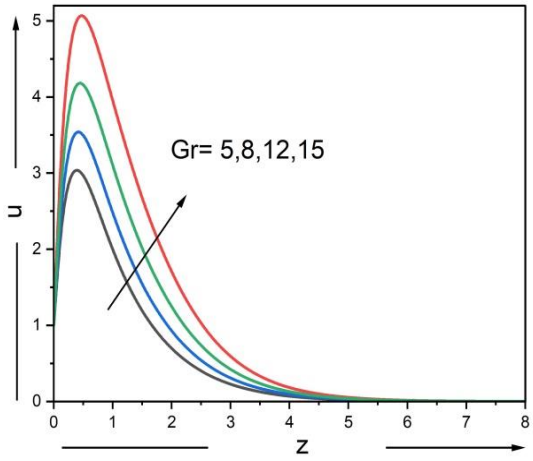

2(E) Velocity portrait for different values of Gr

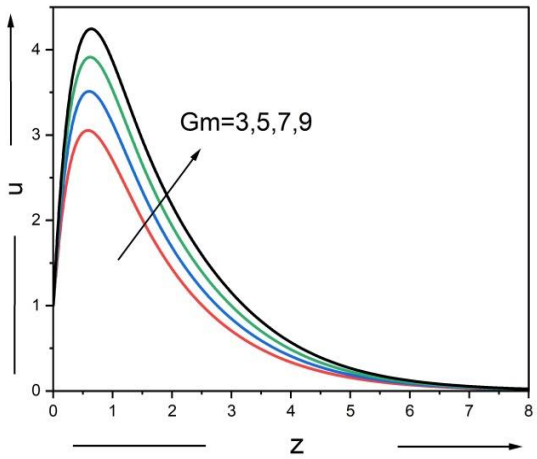

2(F) Velocity portrait for different values of Gm

Figures 2A-F depict velocity portrait

2A Velocity portrait decreases as increase in M since Lorentz forces inception indirection of induced magnetic field offers resistive forces before electrically conducting fluid. Hence momentum boundary layer and flow reduces.

2B Velocity portrait rises with increase in rotation parameter R. This parameter increases the fluid velocity throughout the flow. The effects of acceleration are large near the axis of rotation due to Coriolis force. Hence momentum boundary layer increases with increase in rotation

2C Velocity portrait rises with increase in time t

2D Velocity portrait rises with increase Dufour parameter Du. This increases the parameter velocity and amplifies.

2E Velocity portrait rises with increase in Grashof number Gr depicts velocity profile for Gr, Gm. We observed increase in velocity with increase in potencies of thermal and solute buoyancy forces. Further we observed velocity is large near surfaces and drops quickly to zero.

2F Velocity portrait rises with increase in Grashof number Gm

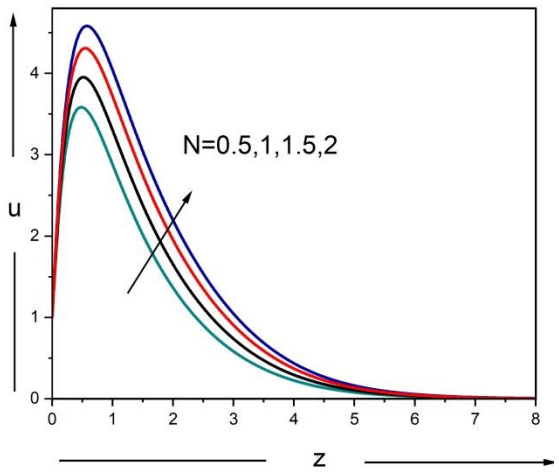

3(A) Velocity potrait for different values of N

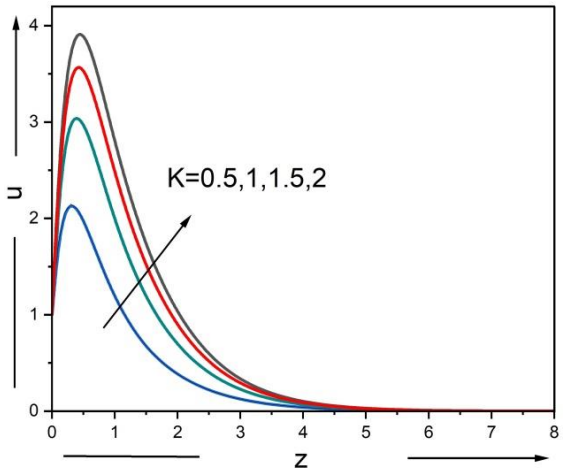

3(B) Velocity potrait for different values of R

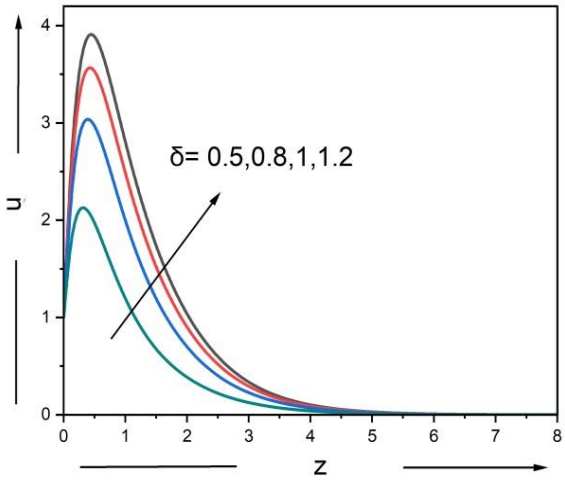

3(C) Velocity potrait for different values of δ

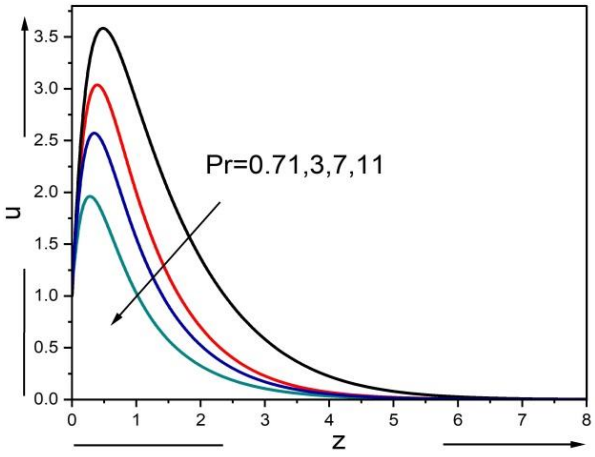

3(D) Velocity potrait for different values of Pr

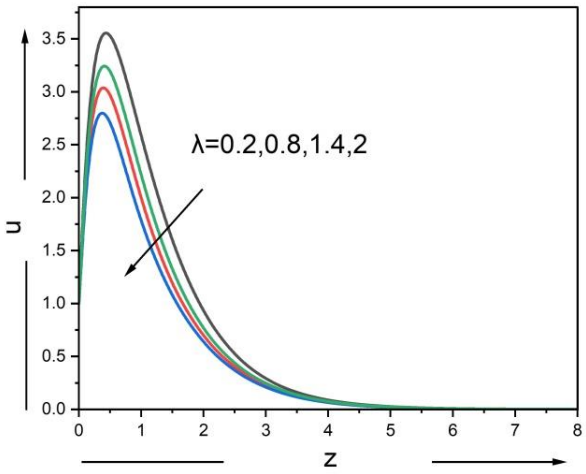

3(E) Velocity portrait for different values of λ

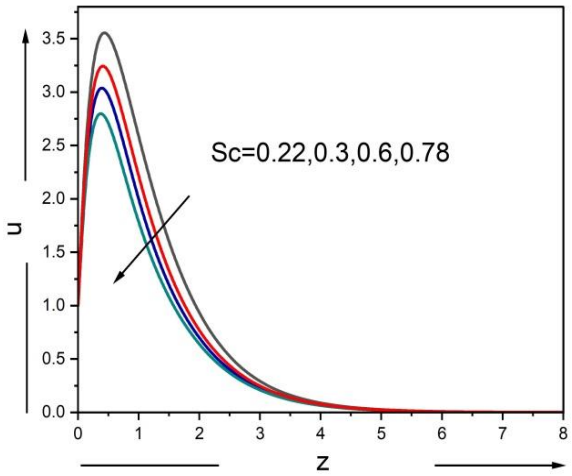

3(F) Velocity portrait for different values of Sc

Figure 3A-F depicts speed of fluid flow

3A Speed of fluid flow rises with growing radiation parameters N. N augments velocity profile with escalation of radiation parameter. Further noticed that speed with which heat is transferred in fluid is enhanced, this results in reducing of viscosity which makes fluid move faster.

3B Speed of fluid flow rises with growing permeability parameter K, This indicates velocity is directly proportional to permeability constant K. Increase in K increase the velocity profile. Whereas inversely proportional to energy and concentration layers.

3C Speed of fluid flow rises with growing material parameter δ. These parameters increase momentum boundary layer thickness in the entire region.

3D Speed of fluid flow decreases with growing prandtl number Pr, increase of Pr makes fluid movement decrease resultant velocity. Highest Prandtl number has high viscosity which makes fluid have substantial thickness

3E Speed of fluid flow decreases with growing viscosity ratio λ

3F Speed of fluid flow decreases with growing Schmidt number Sc. Sc schmidt number choosen were of hydrogen(0.22), helium(0.3), water vapour(0.6), ammonia(0.78) which are observed and found that higher value of Sc means higher bread which results in less of diffusion and hence lessening of speed in fluid region.

Hence boundary layer of momentum thickness decreases by increase in Sc.These parameters decrease thickness of momentum boundary layer.

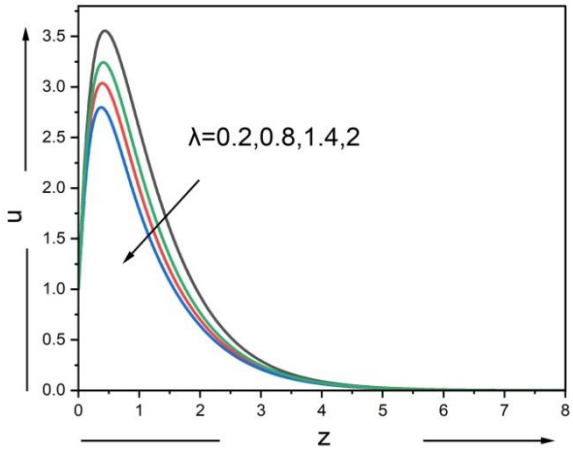

4(A) Velocity portrait for different values of

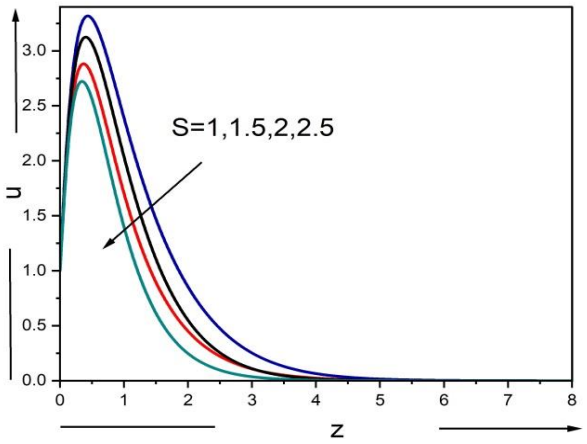

4(B) Velocity portrait for different values of S

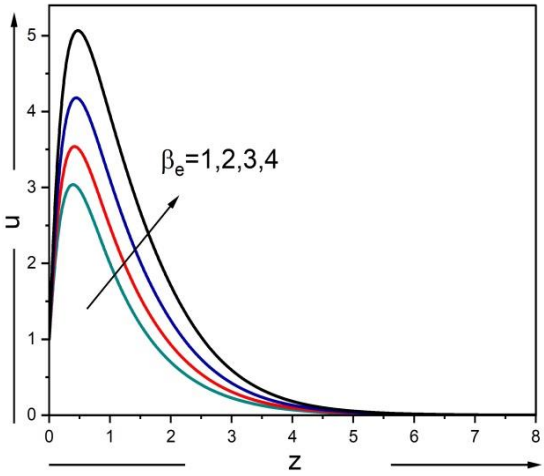

4(C) Velocity portrait for different values of β_e

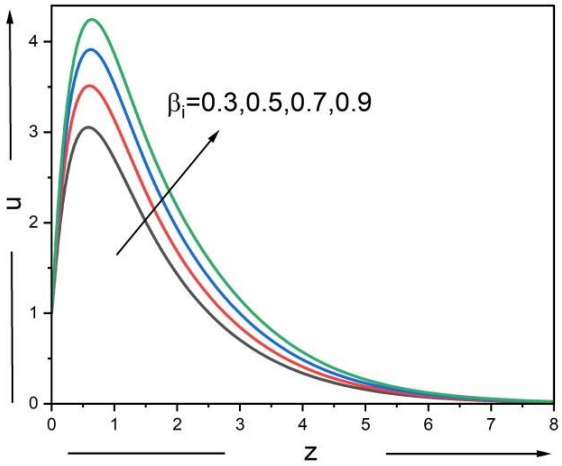

4(D) Velocity portrait for different values of β_i

Figures 4A-D depicts speed of fluid flow

4A Speed of fluid flow at the boundary layer decline with rise in frequentness of oscillation

4B Speed of fluid flow at the boundary layer decline with rise in suction parameter S. S reduces motion boundary layer in the fluid region.

4C Speed of fluid flow at the borderline layer increases with arise in Hall parameter β_e the Hall parameter decreases magnetic fierceness, increases conductibility which in turn augments ion slip parameter. As a result velocity increases.

4D Speed of fluid flow at the borderline layer rise with rise in β_i ion-slip parameter.

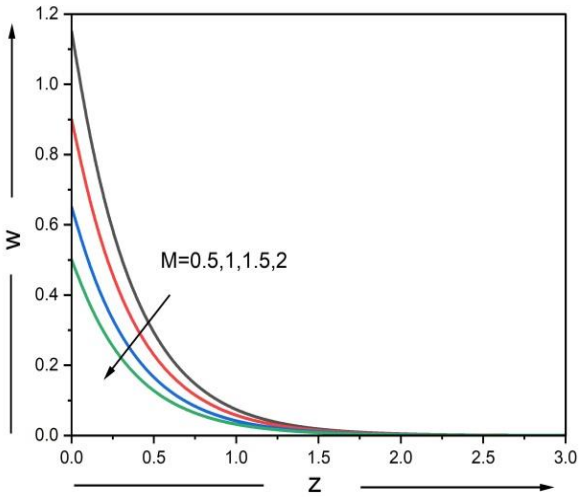

5(A) Micro rotational potrait for different values of M

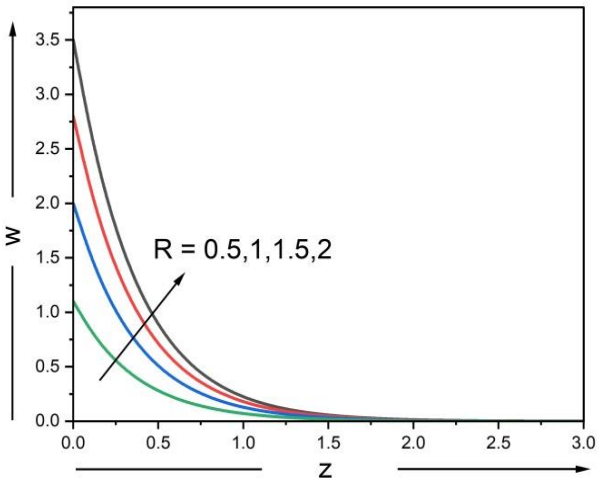

5(B) Micro rotational potrait for different values of R

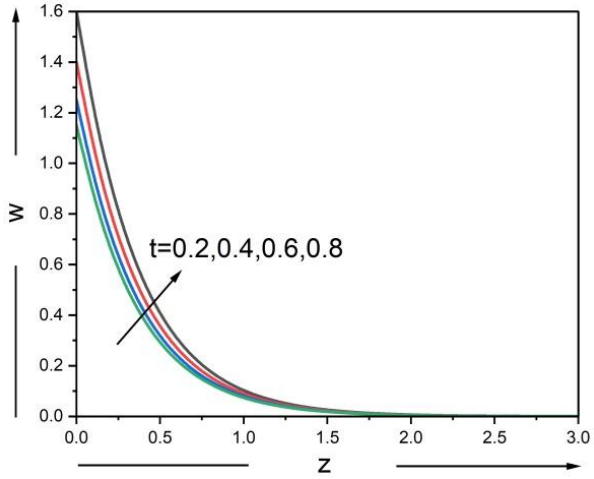

5(C) Micro rotational potrait for different values of t

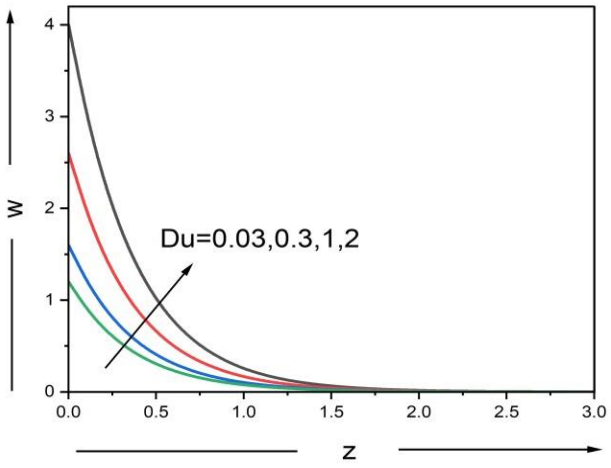

5(D) Micro rotational potrait for different values of Du

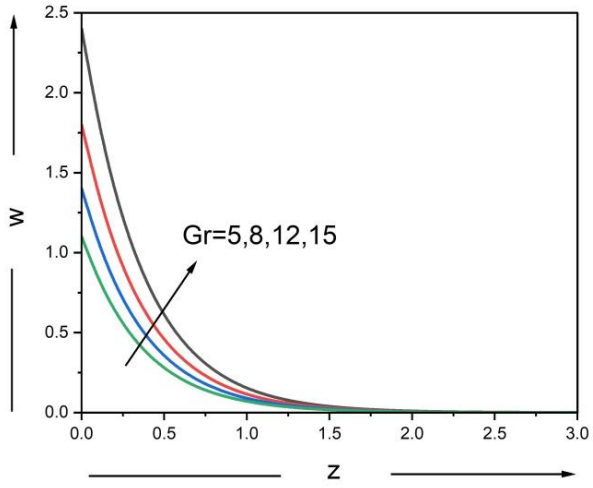

5(E) Micro rotational potrait for different values of Gr

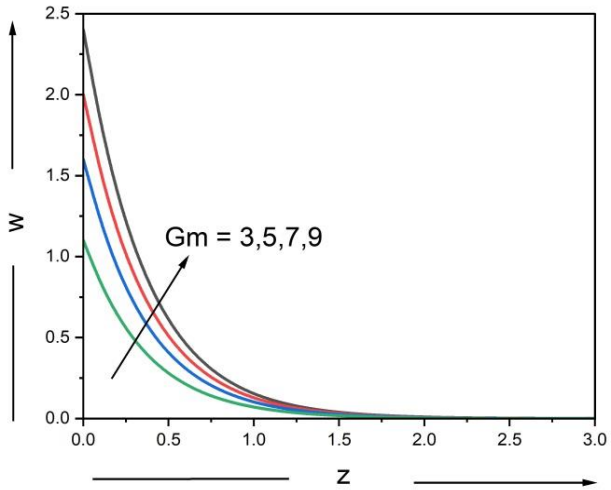

5(F) Micro rotational potrait for different values of Gm

Figures 5A-F depicts micro rotational profile.

5A There is a observation that micro rotational profile decline with rise in Hartmann number M in boundary layer. Not anticipated decrement in speed will be noticed in area by relevance of magnetic field. It is noticed that magnetic field trims down the velocity distribution on all sides. It results in flow tendency not to go along the flow through the flow medium, hence application of magnetic field in permeable material creates decreasing effect will result on velocity variations and thickness of the boundary layer of momentum.

5B Micro rotation profile rises with increase in rotation parameter R. R reduces resulting velocity in fluid region. Hence increase of parameter R results reduction momentum boundary layer.

5C Micro rotation profile rises with increase in time t,

5D Micro rotation profile rises with arise in Du Dufour parameter.

5E, 5F Micro rotation profile rises with rise in Gr thermal Grashof number, Gm mass Grashof number Gm. Velocity of fluids increases with strengthening of solute buoyancy and heat forces, the velocity distribution increases sharply immediately beside to the permeable surface and later there is decay to initial velocity zero smoothly. The reason being buoyancy forces increases both velocity and width of boundary layer of momentum.

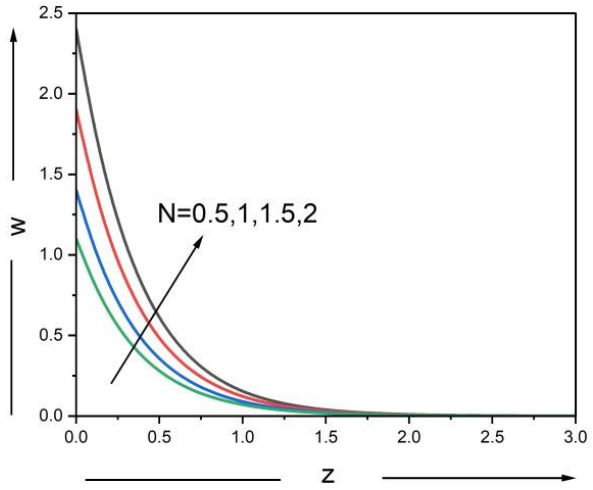

6(A) Micro rotational potrait for different values of N

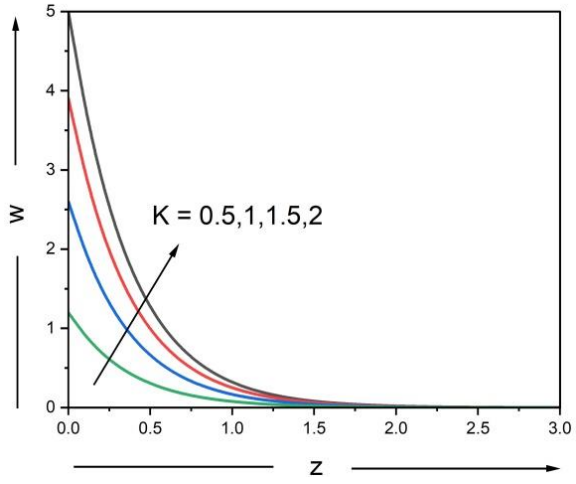

6(B) Micro rotational potrait for different values of K

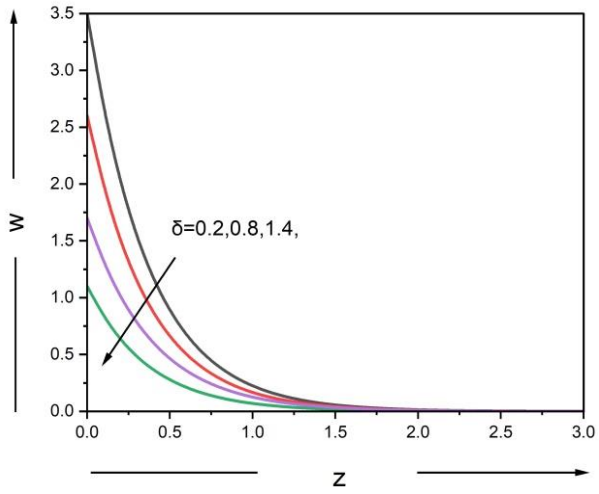

6(C) Micro rotational potrait for different values of δ

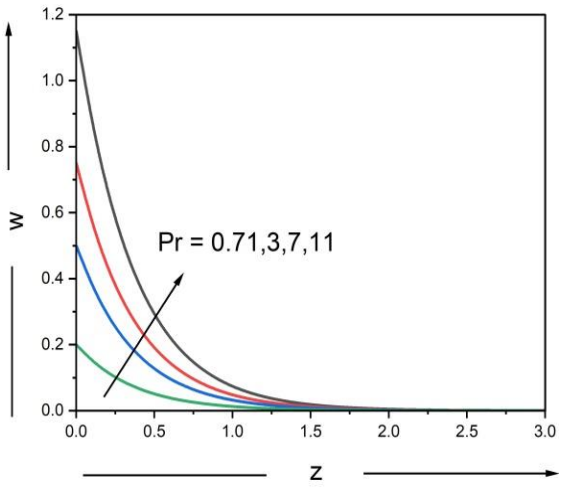

6(D) Micro rotational potrait for different values of Pr

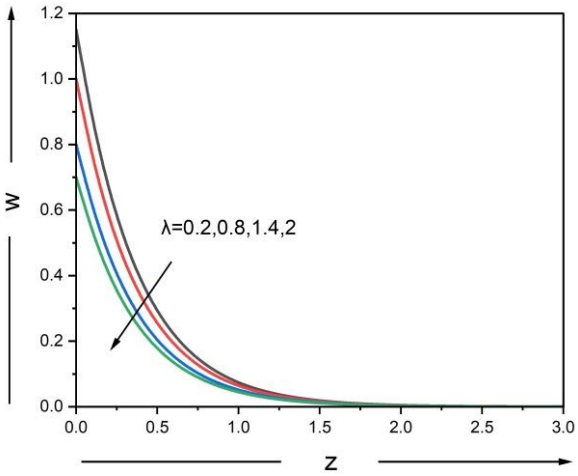

6(E) Micro rotational potrait for different values of λ

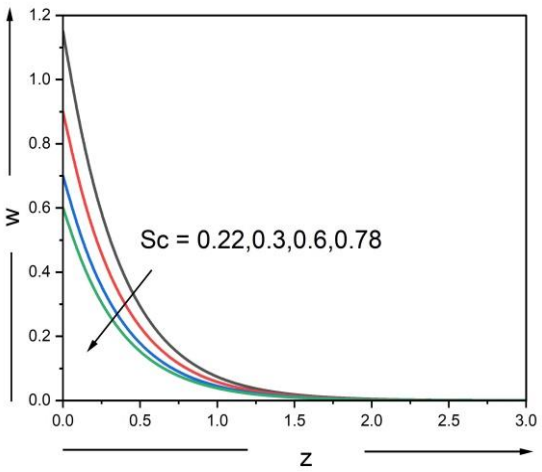

6(F) Micro rotational potrait for different values of Sc

Figures 6A-F depicts micro rotation profile.

6A Micro rotational profile of fluid flow raises with growing radiation parameters N, it is observed that increases in velocity of fluid inside boundary layer due to increase in thermal radiation parameter. Further observed that spike in velocity of fluid boost neary by surfaces to grow mouldl approaching to zero. Hence observed that thickness boundary layer of momentum increases with increase in heat radiation parameter

6B Micro rotational profile of fluid flow raises with growing permeability parameter K. Velocity increases with K growth and then eventually widens the width of the boundary layer of momentum. If ability to penetrate of permeable medium is less it results in speed of fluid to decrease in the flow of the fluid

6C Micro rotational profile of fluid flow raises with growing material parameter δ Increase in parameter increases the velocity of the entire fluid which results in larger thickness in momentum boundary layer.

6D Micro rotational portrait of fluid flow decline with growing prandtl number Pr, increase of Pr makes fluid movement decrease resultant velocity. Highest Prandtl number has high viscosity which makes fluid have substantial thickness

6E Micro rotational portrait of fluid flow decline with growing viscosity ratio λ

6F Micro rotational portrait of fluid flow decline with growing Schmidt number Sc. Increase in Schmidt number inclines to decrease velocity distribution .Also noticed that increase in Schmidt number results in reduction of

thickness boundary layer of momentum

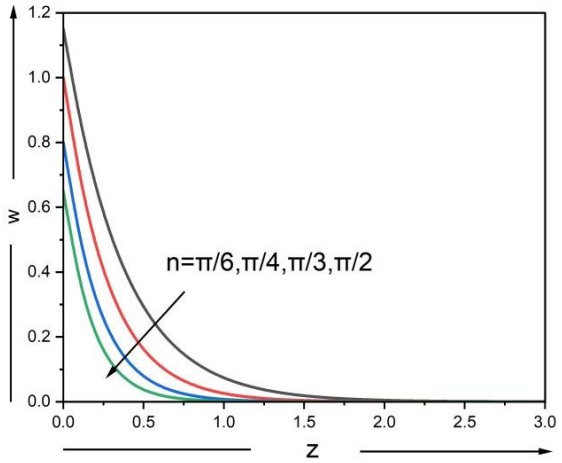

7(A) Micro rotational potrait for different values of n

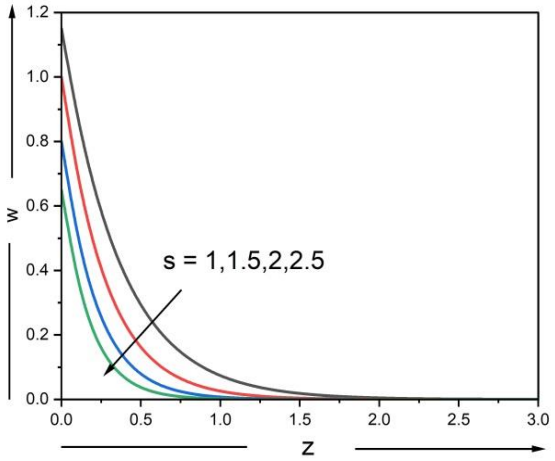

7(B) Micro rotational potrait for different values of S

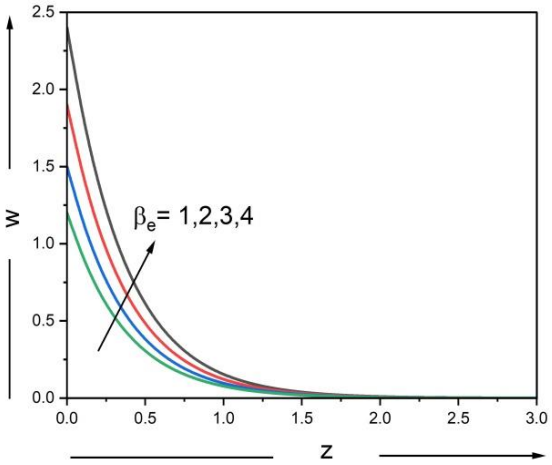

7(C) Micro rotational potrait for different values of β_e

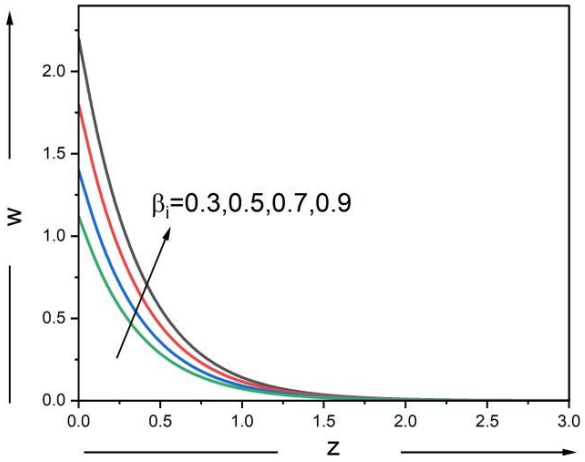

7(D) Micro rotational potrait for different values of β_i

Figures 7A-D depicts micro rotational profile

7A Micro rotational profile decreases with rise in frequency of oscillation.

7B Micro rotational profile decreases with rise in suction parameter S. Increase in suction parameter dreceases the velocity of the entire fluid which results in reduction of thickness in momentum boundary layer.

7C Micro rotational profile increases with rise in Hall parameter β_e. Increase of velocity with increase of Hall parameter.

7D Micro rotational profile increases with rise in ion-slip parameter β_i. depicts influence of ion slip parameter on w which increases with increase in ion slip parameter,since damping forces decreases velocity increases in the flow direction

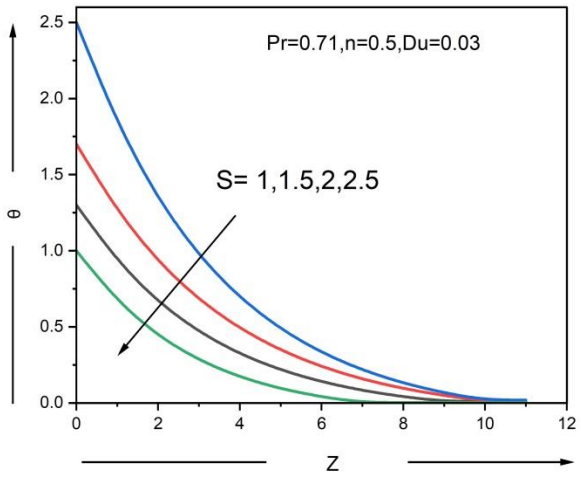

8(A) Temperature profile for different values of S

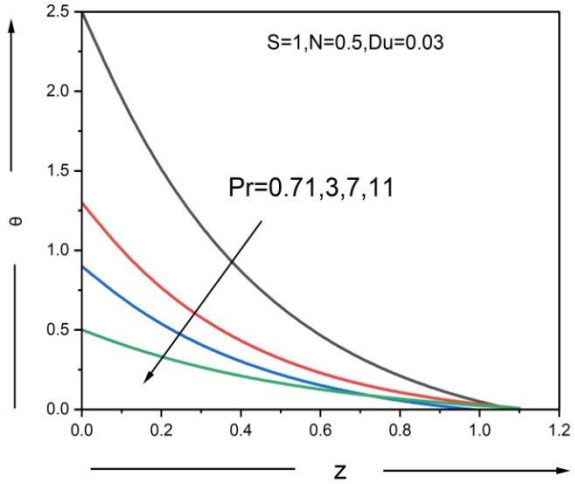

8(B) Temperature profile for different values of Pr

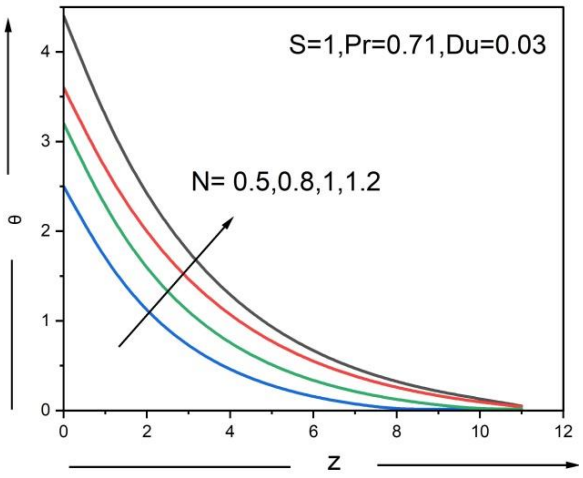

8(C) Temperature profile for different values of N

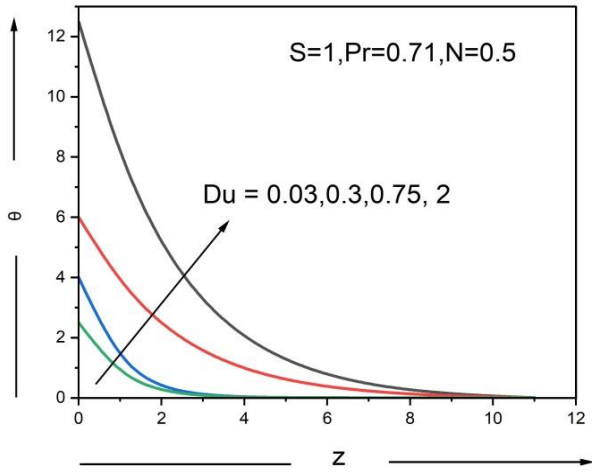

8(D) Temperature profile for different values of Du

Figure 8A-D depicts temperature profile for not similar parameters like Prandtl number Pr, Dufour parameter Du, radiation parameter N, suction parameter S.

8A Temperature profile reduces with growing suction parameter S. Thermal boundary layer thickness reduces with rise in S, hence temperature profile decreases.

8B Temperature profile reduces with growing Prandtl parameter Pr, increase of Pr makes fluid movement decrease thermal temperature. Highest Prandtl number has high viscosity which makes fluid have substantial thickness of energy boundary layer

8C Temperature profile enhances with rise in N and density of thermal boundary layer increases throughout the fluid region.

8D Temperature profile enhances with increase in Du. Thermal boundary layer thickness increases with increase in Du hence temperature profile sees an increase.

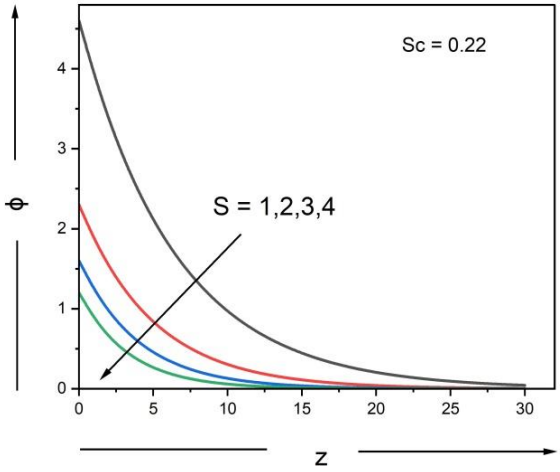

9(A) Concentration profile for different values of S

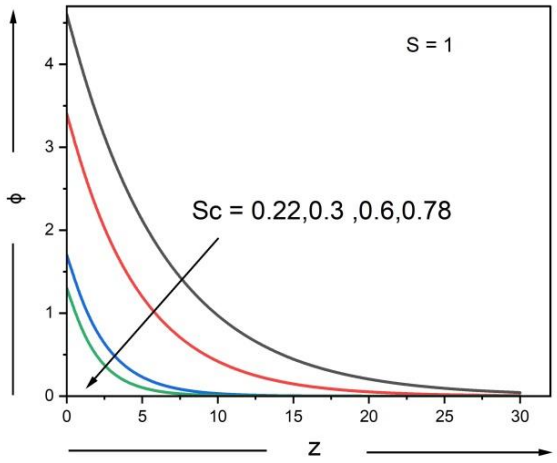

9(B) Concentration profile for different values of Sc

Figures 9A, B depicts mass Concentration profile

9A Concentration of liquid decreases with rise in suction parameter S depicts concentration profile for S, The concentration profile decrease with increase in suction parameter S and chemical reaction parameter.

9B Concentration of liquid decreases with rise in Schmidt number Sc depicts concentration profile for Schmidt number Sc. Sc increase the fluid flow throughout region hence decreases concentration profile.

TABLE 1 Skinfriction and couple stress coefficient (t = 0.2)

M	R	Du	Gr	Gm	N	K	Pr	λ	δ	Sc	S	n	β_e	β_i	C_f	C_w	Present ResultsC_f	Present ResultsC_w
0.5	0.5	0.03	5	3	0.5	0.5	0.71	0.2	0.5	0.22	1	π/6	1	0.3	0.360704	15.2439	0.360715	15.243912
1															0.344574	13.7022	0.344586	13.702209
1.5															0.322987	11.7811	0.322999	11.781113
	1														0.345387	13.6405	0.345397	13.640505
	1.5														0.332429	12.1493	0.332441	12.149301
		0.3													0.487331	20.6016	0.487345	20.601611
		1													0.81563	34.4921	0.81576	34.492109
			8												0.468522	19.8056	0.468534	19.805614
			12												0.612386	25.8925	0.612398	25.892509
				5											0.509415	21.5359	0.509426	21.535914
				7											0.658162	27.8294	0.658174	27.829416
					1										0.453352	19.1639	0.453363	19.163909
					1.5										0.548025	23.1695	0.548037	23.169508
						1									0.403313	19.9498	0.403325	19.949811
						1.5									0.417904	21.9943	0.417916	21.994309
							3								0.214603	9.06269	0.214615	9.0626912
							7								0.198803	8.39433	0.198814	8.3943309
								0.4							0.37556	14.2483	0.37567	14.248308
								0.6							0.388218	13.412	0.388229	13.41209

TABLE 1 continued

M	R	Du	Gr	Gm	N	K	Pr	λ	δ	Sc	S	n	β_e	β_i	C_f	C_w	Present ResultsC_f	Present ResultsC_w
0.5	0.5	0.03	5	3	0.5	0.5	0.71	0.2	0.5	0.22	1	π/6	1	0.3	0.360704	15.2439	0.360715	15.243912
									0.8						0.354004	9.43158	0.354016	9.4315812
									1						0.350813	7.5077	0.350824	7.507711
										0.3					0.291538	12.3175	0.29155	12.317507
										0.6					0.200019	8.44535	0.20003	8.4453506
											2				0.190298	12.0906	0.190309	12.090611
											3				0.089608	6.62875	0.089619	6.628751
												π/4			0.356212	15.2442	0.356223	15.24421
												π/3			0.349823	15.2449	0.349834	15.244909
													2		0.363246	15.4937	0.363257	15.493714
													3		0.364413	15.6093	0.364425	15.609316
														0.5	0.361142	15.2873	0.361153	15.287313
														0.7	0.36156	15.3285	0.361572	15.328515

TABLE 2 Comparative results of Nu (Kc = 0, Q = 0)

S	N	Du	Pr	Olajuwon and Oahimire[8]	Veerakrishna[18]	Present
1	0.5	0.03	0.71	1.025446	1.025443	1.025445
2				2.335568	2.335565	2.335567
3				3.699857	3.699854	3.699856
	0.8			0.588749	0.588748	0.588749
	1			0.144155	0.144153	0.144154
		0.3		0.854748	0.854746	0.854748
		0.75		0.699857	0.699854	0.699855
			3	0.985547	0.985544	0.985546
			7	0.885478	0.885476	0.885477

TABLE 3 Comparative results of Sh (Kc = 0)

S	Sc	Olajuwon and Oahimire[8]	Veera Krishna[18]	Present
1.0	0.22	0.22000	0.22000	0.22000
2.0		0.44000	0.44000	0.44000
3.0		0.66000	0.66000	0.66000
	0.30	0.30000	0.30000	0.30000
	0.60	0.60000	0.60000	0.60000

The values obtained for Nusselt number and skin friction coefficient are corroborated by comparing with MATLAB code and numerical scheme with analytical values, considering Ec=0.The values tabled by Satya Narayana et al.[12] are in good harmony with values in Table 1 and 2.Hence with immense confidence the values obtained by the code for numerical results are considered as excellent solution for the problem in the paper.

Finite element method is very popular in modern engineering sciences and applied to study non-Newtonian fluids. In Table 3 we tabled solutions of Sherwood number obtained with small perturbation and Finite Element Method . By comparison between values, the conclusion obtained is fine correlation and reliance is high on Finite Element Method. The combination of Finite Element Method and MATLAB is very accurate to study the model for all its parameters.

The values are obtained for Nusselt number, Sherwood number, local skin friction coefficient and wall couple stress coefficient by Galerkin finite element method and weighted residual method. The values obtained by analytical methods listed in Das[13] are compared with these values and are tabled in Table 1.The comparison is done in absence of M=0, Q=0,Ec=0. Also in Table 3 comparison of analytical values obtained by Satya Narayana et al.[12] considering Ec=0 is done with Galerkin finite element method and weighted residual method. Results obtained are in excellent agreement with results existing and is of immense confidence.

5. Conclusions

We studied problem free convective MHD unsteady incompressible micro polar mass and thermal transfer flow of fluid past partially-infinite perpendicular porous moving plate in steady permeable medium.

The problem is studied with exhaust and in company of thermal radiation, thermo-diffusion, ion slip and Hall effects.
The conclusions of research are

1. The speed of fluid flow and micro rotation decline with rise in S suction parameter. Speed of fluid Increases with rise in Du Dufour number, R radiation parameter, Hall and ion slip parameter.
2. The momentum borderline layer density decreases with rise in viscosity ratio and increases with increase in Material parameter (variable).
3. The heat of the fluid increases with increase in radiation parameter and dufour number whereas heat of fluid decline with increase in Prandtl number and suction variable.
4. The concentration of fluid decline with rise in suction parameter and Schmidt number.

. REFERENCES

[1] Eringen AC. Theory of micropolar fluids. J Math Mech.1966; 16:1-18.

[2] Ellahi R, Bhatti MM, Pop I. Effects of Hall and ion-slip on MHD peristaltic flow of Jeffrey fluid in a non-uniform rectangular duct. IntJ Numerical Method Heat Fluid flow.2016;26(6):1802-1820.

[3] Bhatti MM, Abbas MA,Rashidi MM. Effect of Hall and ion slip on peristaltic blood flow of Eyrig Powell fluid in a non-uniform porous channel. World J model Simul. 2016; 12(4):268-279.

[4] Srinivasacharya D, Shafeeurrahman Md. Hall and ion-slip effects on mixed convection flow of Nano fluid between two concentric cylinders. J Assoc Arab Univ Basic Appl Sci. 2017; 24(1):223-231.

[5] Jitendra KS, Srinivasa CT. Unsteady natural convection flow of a rotating fluid past an exponential accelerated vertical plate with Hall current, ion-slip and magnetic effect. Multidiscip Model Mater Struct.2018;14(2):216-235.

[6] Veera Krishna M, Chamkha AJ. Hall and ion slip effects on MHD rotating boundary layer flow of Nano fluid past an infinite vertical plate embedded in a porous medium. Res Phys. 2019;15: 102652.

[7] Sara IA, Bhatti MM. The study of non –Newtonian nanofluid with Hall and ion-slip effects on peristaltic ally induced motion in a non-uniform channel. RSC Adv. 2018;8:7904-7915.https://doi.org/10.1039/c7ra13188g

[8] Olajuwon BI, Oahimire JI. Unsteady free convection heat and mass transfer in an MHD micro-polar fluid in the presence of thermo-diffusion and thermal radiation. Int J Pure Appl Math.2013; 84(2):15-37. https://doi.org/10.12732/ijpam.v84i2.2

[9] Ganapathy R. A notes on oscillatory Couette flow in a rotating system.J Appl Mech. 1994;61: 208-209.

[10] Brewster MQ. Thermal Radiative Transfer and Properties 12. Hoboken, NJ: John Wiley & Sons; 1972:6-9.

[11] Sutton G, Sherman A. Engineering Magneto hydrodynamics. New York: Mc Graw Hill; 1965.

[12] MD Shamshuddin, Thumma Thirupathi, P.V.Satya Narayana. Micropolar Fluid Flow Induced due to a Stretching Sheet with Heat Source/Sink and Surface Heat Flux Boundary Condition Effects, Journal of Applied and Computational Mechanics.2019;5:816-826.

[13] K.Das, Slip effects on heat and mass transfer in MHD micropolar fluid flow over an inclined plate with thermal radiation and chemical reaction, International Journal for Numerical Methods in Fluids.2012;70:96-113.

[14] Ch.Vijaya Bhaskar, Siva Reddy Sheri, Anjan Kumar Suram, "Numerical analysis of MHD casson fluid flow over an exponentially accelerated vertical plate in embedded porous medium with ramped wall temperature and ramped surface concentration in uniform magnetic field," International Journal of Applied Power Engineering (IJAPE), vol. 9, No. 2, , pp. 89-99, August 2020.

[15] M. Ijaz Khan , Faris Alzahrani , Aatef Hobiny , "Heat transport and nonlinear mixed convective nanomaterial slip flow of Walter-B fluid containing gyrotactic microorganisms,"Alexandria Engineering Journal 59,1761-1769,2020.

[16] Krishna MV, Ameer Ahamad N, Chamkha AJ. Hall and ion slip effects on unsteady MHD free convective rotating flow through a saturated porous medium over an exponential accelerated plate. Alex Eng J. 2020; 59:565- 577. https://doi.org/10.1016/j.aej.2020.01.043

[17] Singh JK, Vishwanath S. Hall and induced magnetic field effects on MHD buoyancy driven flow of Walters'B fluid over a magnetized convectively heated inclined surface. Int J Ambient Energy. 2021. https:// doi.org/10.1080/01430750.2021.1909652.

[18] M.Veera Krishna, Hall and ion slip effects on MHD free convective rotating flow bounded by the semi-infinite vertical porous surface(2020) 1-19, https://doi.org/10.1002/htj.21700.

[19] M.Veera Krishna, C.S.Sravanthi, R.S.R.Gorla, Hall and ion slip effects on MHD rotating flow of ciliary propulsion of microscopic organism through porous media, Int. Commum. Heat Mass Tran. 112(2020)104500, https://doi.org/10.1016/j.icheatmasstransfer.2020.104500

[20] Olanrewaju A.M., Makinde O.D, Boundary layer stagnation point flow of a Nano fluid over a permeable flat surface with Newtonian Heating, Chem.Eng.Commun. 2013: 200(6):836-852

[21] Pit R. Hervet H and Leger. L Direct experimental evidence of slip in hexadecane: solid interfaces, Phys.Rev.Lett. (2000): 85 980- 983

[22] Sheikholeslami, M., Darzi, M. and Li, Z. (2018), "Experimental investigation for entropy generation and energy loss of Nano-refrigerant condensation process", International Journal of Heat and Mass Transfer, Vol. 125, pp. 1087-1095.

[23] Reza, F., Mebarek-Oudina, F. and Makinde, O.D. "MHD slip flow of Cu-Kerosene Nano fluid in a

channel with stretching walls using 3-stage Lobatto IIIA formula", Defect and Diffusion Forum, (2018): Vol. 387, pp. 51-62

[24] Heat and Mass Transfer Fundamentals & Application 2015 'McGraw-Hill Book Company New York'

[25] Bathe KJ 1996 'Prentice Hall-New Jersey'

[26] Reddy J N 2006 'McGraw-Hill Book Company New York'